COMITATO NAZIONALE PER L'ENERGIA NUCLEARE
Laboratori Nazionali di Frascati

LNF-76/40(R)
30 Giugno 1976

R. Camilloni, A. Giardini Guidoni, G. Missoni, G. Stefani, G. Tiribelli and D. Vinciguerra: VALIDITY OF THE (e, 2e) REACTIONS AS A PROBE OF THE ATOMIC AND MOLECULAR STRUCTURE.

Servizio Documentazione
dei Laboratori Nazionali di Frascati del CNEN
Casella Postale 70 - Frascati (Roma)

Laboratori Nazionali di Frascati
Servizio Documentazione

LNF-76/40(R)
30 Giugno 1976

R. Camilloni[x], A. Giardini Guidoni, G. Missoni[o], G. Stefani[x], R. Tiribelli, and D. Vinciguerra: VALIDITY OF THE (e,2e) REACTIONS AS A PROBE OF THE ATOMIC AND MOLECULAR STRUCTURE. -

ABSTRACT

Results of an extensive set of measurement of (e,2e) reactions on noble gases are reported, along with a coincise description of the experimental set-up. Some conclusions on the conditions in which the (e,2e) reactions are valuable tool to investigate atomic wave functions are drawn.

1. - INTRODUCTION. -

It is by now commonly accepted that, among the various processes induced by a beam of fast electrons colliding with atomic or molecular targets, those in which ionization occurs and two fast electrons emerge at large angles and are detected (the(e,2e)reactions), give valuable information on the electronic properties of atoms and molecules[1-6]. Measurements on (e,2e) rections have been carried out both on atoms and molecules in a variety of experimental conditions in the few laboratories active in the field [1,2,7,8], however as pointed out in the recent review by Mc Carthy and Weigold[4] the study of these reactions is still under development, and there is no consensus on the best experimental conditions needed to obtain as much information as possible on the atomic structure. The possibility to obtain such information is linked to the validity of the model used in describing the scattering process and in particular to the correct interpretation of the experimental data. In this paper, along with a concise review of the theoretical model and experimental set-up, we report an extensive series of measurements carried out on noble gases with the aim to check the theory and to find experimental conditions in which the (e,2e) reactions can provide reliable information on atomic and molecular structures.

2. - THE PROCESS. -

The (e,2e) are reactions of electron impact ionization in which the kinematics of the process is fully determined by measuring the momentum vectors of the initial and final electrons. In fig. 1 the kinematics of the experiment in the laboratory system is shown: $\bar{p}_o$ is the momentum of the incident electron, $\bar{p}_1$ and $\bar{p}_2$ are the momenta of the two outgoing electrons and $\bar{p}_R$ is the momentum of the residual ion R.

Conservation of the energy and momenta can be written as:

$$E_o - B_{nl} = E_1 + E_2 + E_R \qquad (1a), \qquad \bar{p}_o = \bar{p}_1 + \bar{p}_2 + \bar{p}_R \qquad (1b)$$

(x) - Laboratorio Metodologie Avanzate Inorganiche del CNR, Via Montorio Romano, Roma (Italy).
(o) - Laboratorio Ricerche di Base SNAM Progetti, Monterotondo, Roma (Italy)

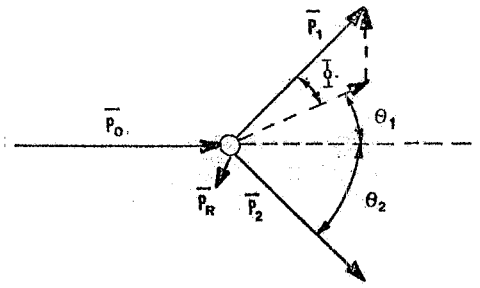

Fig. 1 - Schematic representation of an (e, 2e) reaction

where E_o and E_1, E_2 are the kinetic energies of the incident and outgoing electrons and E_R is the recoiling ion energy. [2] Since the latter is always negligible, the total energy of the final electrons can be related to the binding energy of the initially bound electron B_{nl} by simplifying the relationship (1a):

$$B_{nl} = E_o - (E_1 + E_2) \tag{2}$$

For such a reaction to provide structural information on the atomic target some basic assumptions on the way in which the interaction take place must be done; these assumptions are correlated and refer: firstly (1a) to the reaction mechanism which must be a direct two-bodies interaction and, secondly, to the very nature of the system under study, where it is assumed that the many body effects do not deprive the concept of single particle state of any physical meaning.

If the kinetic energies of the free electrons are made very large compared to the binding energy B_{nl}, and the momentum transfer is also large compared to the characteristic momentum $\langle q \rangle$ of the bound electron, the target binding forces can be expected not to play any role in the scattering and hence Impulsive Approximation should then apply.

The validity of the second hypothesis depends only from the particular target and can be considered true for closed shell system as noble gases.

To bring the experimental data to a full significance it is further necessary to account for the residual interaction that the "interacting electrons" have with the spectator residual ion. It has been shown [9] that, when the atomic potential is a slowly varying function of the coordinates in the main part of the interaction region, the overall matrix element of the process is given in the form:

$$M_{if} = \Sigma_{|q\rangle} \langle \chi^-_{k_1} \chi^-_{k_2} | t_c | \chi^+_{k0} q \rangle \langle q \, \psi_R | \psi_A \rangle \tag{3}$$

in which a two particle transition matrix has been factorized out. Multiple scattering of the incoming and outgoing electrons in the atomic field has been neglected. The $\langle \chi_{ki} |$ in (3) are electron wave functions which, in a first approximation, are treated as plane waves, while $| t_c |$ is the on shell matrix element for the Coulumb e-e scattering, and ψ_R and ψ_A are respectively the residue and the atomic wave function.

According to the I. A. which implies the conservation of the momentum of the residual ion during the interaction, the q value in (3) must be understood as the momentum of the bound electron before interaction, since then results $+\vec{q} = -\vec{p}_R$. As to atomic wave functions if they are expressed by a product of antisimmetrized one electron w.f.s (H. F. w. f.) or a C. I. expansion of H. F. w. f.s., the overlap integral $\langle q \, \psi_R | \psi_A \rangle$ further splits into the Fourier transform $\langle q \, \varphi_{nl}(\vec{r}) \rangle = \varphi_{nl}(\vec{q})$ of the bound electron w. f., which give rise to the observed momentum distribution (e. m. d.), times the overlap integral $\langle \psi_R | \psi_{A-1} \rangle = (K^I_{nl})^{1/2}$ which accounts for the satellite structure observed in the energy spectra [2, 5].

Calculation of the scattering cross section in this plane waves impulse approximation (P. W. I. A.) leads to the formula:

$$\frac{d^5\sigma}{d\Omega_1 d\Omega_2 dE_1} \propto \left| \langle k_1 k_2 | t_c | k_o \, q \rangle \right|^2 \left| \varphi_{nl}(\vec{q}) \right|^2 K^I_{nl} \tag{4}$$

When the energies of the electrons involved in the scattering are not sufficiently large as compared with the atomic potential, distortion of the electron waves takes place. A suitable optical potential[2] is introduced to account for this effect with the result that the $\langle \chi_{ki} |$ are no longer momentum eigenstates.

These modifications correspond to describing the scattering inside the potential well of the atom, where the electrons momenta are larger than those measured outside. Nevertheless in the D. W. I. A. the overall matrix element can still be given by the product of a two electron direct scattering matrix, which is now computed off the energy shell, times a distorted momentum distribution. A simple way to compute this distortion has been introduced by Mc Carthy and coworkers[2, 4]; this eikonal approximation gives the following form for the electrons w. f. :

$$\chi^{\pm}_{k} \propto e^{\pm i(1+\beta+i\gamma)\bar{k}\cdot\bar{r}} \qquad (5)$$

where $\beta = V/2E$ is a real parameter proportional to the effective potential experienced by the electrons and γ is an attenuation factor affecting almost only the absolute value of the cross section. The effect of β is to change the value of the momentum.

In summary two kinds of spectra can be obtained from the (e,2e) experiments: i) The energy spectrum obtained by varying the incident electron energy while keeping the angles and energies of the outgoing electrons fixed. The peaks observed in this way correspond to the various separation energies of the final ionic states. ii) The angular distribution obtained, for instance, at constant value of the initial and final electron energies and by varying the scattering angles : in this way a particular final ionic state can be selected and, from the shape of tha angular distribution the function $|\varphi_{nl}(\bar{q})|^2$ can be deduced.

3. - EXPERIMENTAL . -

Except for minor modification the apparatus used in these studies is the same that was previously described.[5] For completeness its features and its performances will be briefly reviewed here. It mainly consists of a stainless steel cylindrical chamber 60 cm high and 130 cm in diameter, connected with the pumping system. All the basic components: the electron gun, the two rotatable electron spectrometers and the gaseous target, are placed on the lower flange, which can easily removed from the chamber. A picture of the flange where it is possible to identify these main components is shown in fig. 2a.

The pump system consists of a rotary mechanical pump, an 8000 lit. sec. mercury diffusion pump, and two baffles refrigerated with water and liquid nitrogen respectively. It provides a typical background pressure rises to about 10^{-6} torr. An He criopump (11) sitting on the top flange in front of the jet is sometime used.

The electron gun, a Varian Auger model, provides a quite well collimated ($\Delta\vartheta$ about 4×10^{-2} rad.) electron beam in the energy range 50 - 3000 eV. Beam intensity is from few μA to 200 μA.

The gaseous beam is obtained by allowing the gas to effuse through a Bendix multichannel array whose thickness is .25 mm. Each channel is 10μi. d. and the active area is about 50% of the total. The multichannel is sealed on an hypodermic needle 0. 6 mm. i. d. placed about 3mm below the electron beam path. The intersection of the two beams defines an interaction volume of about 2 mm^3 in the center of the chamber. Gas density in the interaction region is estimated to be about 5×10^{-3} torr.

The two identical electron spectrometers are fixed to rigid supports independently movable on a circular path around the interaction volume on a plane containing the electron beam path. In this coplanar arrangement, the azimuthal angle Φ is equal to zero and the angles ϑ_1 and ϑ_2 (see fig. 1) can be independently varied from 28° to 72°. The motion provided from the outside by Riber rotary manipulators, allows for a positioning precise to $\pm$ .2° . The spectrometers are hemispherical electrostatic analyzers formed by two concentric hemispheres of 105mm. and 135mm./ diameter respectively. Entrance and exit slits are made by molibdenum diaphragms

3 mm i. d. Fringing fields are reduced by Herzog elements 15 mm. long placed at the entrance and exit of the hemispheres. The energy resolution of each spectrometer can be varied by means of plane decelerating lenses down to a minimum value of 1, 9 eV (FWHM). Electron detectors are Bendix channeltron multipliers. The performance of each electron spectrometer was tested by measuring the angular distribution of elastically scattered electrons on some noble gases[10].

The data acquisition system is very similar to the previously described one [1, 10]. Its main components are shown in fig. 2b.

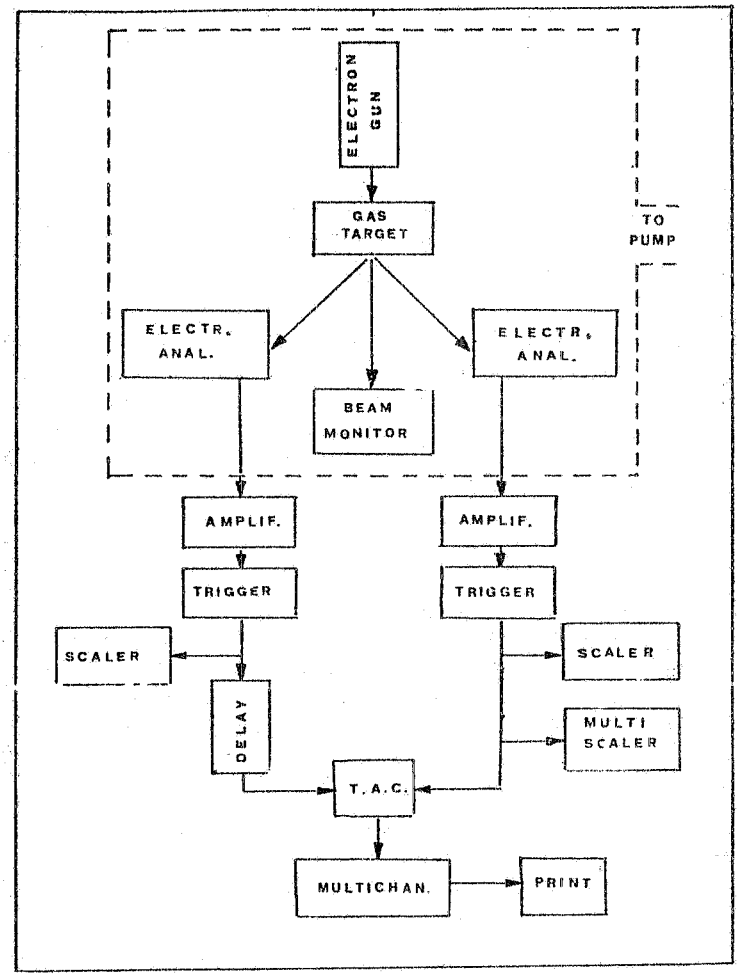

Fig. 2b - Block diagram of experimental set-up.

4. - RESULTS AND DISCUSSION.

In the following we report a series of measurements of angular distribution taken on noble gases for incoming electrons energies ranging from 200 up to 2600 eV. The data are compared with curves computed from the two above mentioned theoretical models P. W. I. A. and D. W. I. A. in the eikonal approximation as given in papers (2-4), where the value of the attenuation factor γ has been set equal to zero hence neglecting any absorption effect. The factor $\beta = V/2E$, and therefore V, has been used as a parameter. The H. F. atomic wave functions used in calculating the form factor in the expression (4) have been taken from Clementi and Roetti[12]. The theoretical curves have been computed by folding in the angular and energy resolution of the apparatus with expression (4) and have been normalized not to the area but to the peak value of the experimental distribution, in order to avoid uncertainties connected with the unmeasured tails. In the figs. 3 to 7 we report the measured angular distribution of the electrons ejected in the He 1s ionization, for a

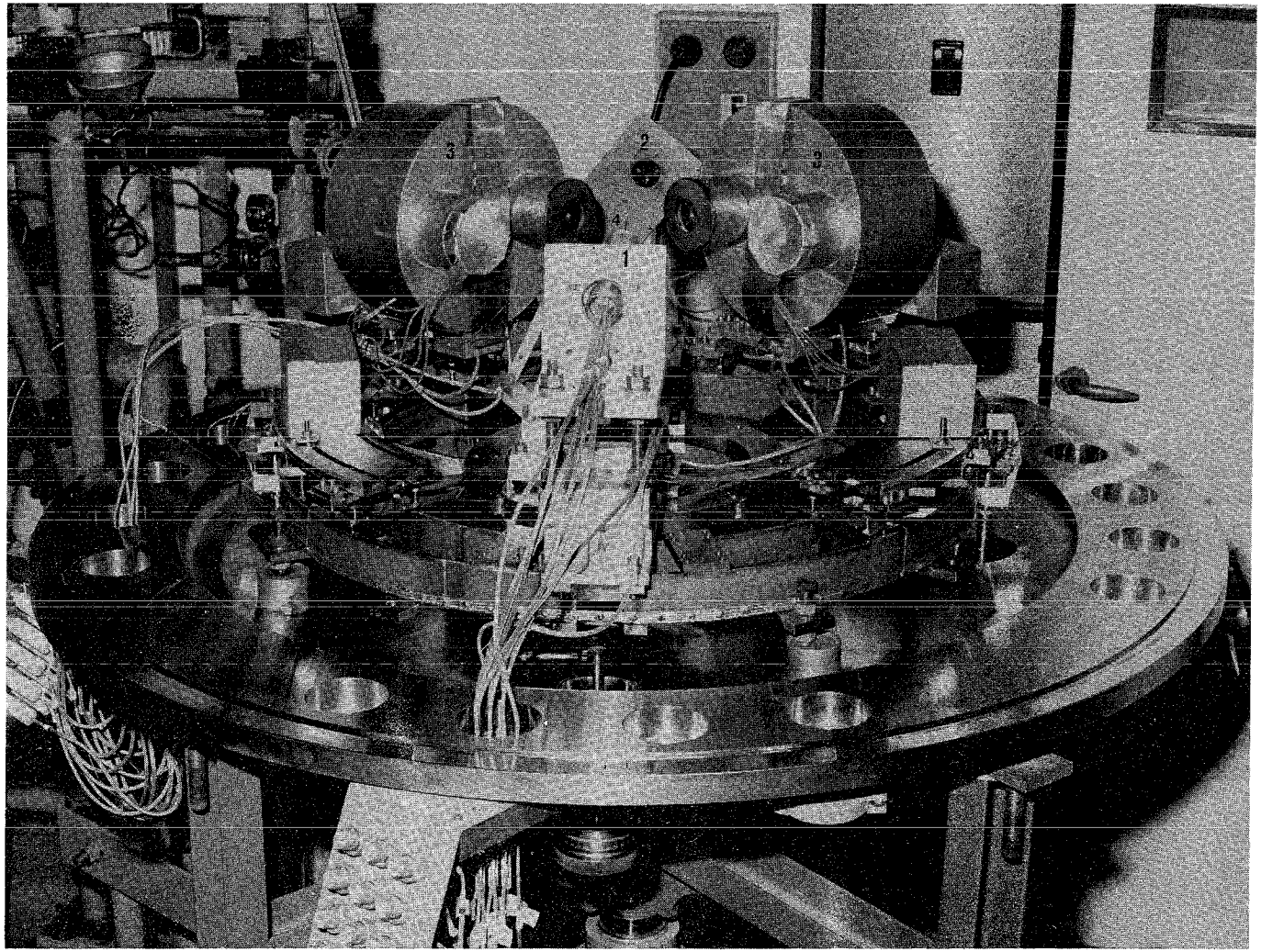

FIG. 2a - Picture of the apparatus for (e, 2e) reactions. (1) Electron Gun, (2) Faraday cage, (3) Electron spectrometers, (4) Multichannel array.

number of incident electrons energies, together with the theoretic previsions. All the measurements have been performed in the symmetrical coplanar geometry, by setting $E_1 = E_2 = (E_o - B_{nl})/2$, $\vartheta_1 = \vartheta_2$ so that only values of the momentum q parallel to the direction of the incoming electron are selected through the relationship $q = (2p \cos\vartheta - p_o)\hat{p}$ folded in with the apparatus resolution.

The shift and asymmetry of the curves respect to 45^o is due to the strong dependence of the cross section on the scattering angle. According to the peculiar character of the s type orbital a maximum in the angular distribution, corresponding to a value $q \simeq 0$ of the bound electron, is clearly shown.

In the low energy range (200 and 400 eV), as can be seen in fig. 3 and 4, both the P. W. I. A. (equivalent to V=0 in D. W. I. A.) and the D. W. I. A. eikonal appear unable to predict the position of the maximum as well as the width of the angular distribution. The effect of having introduced the parameter V in the D. W. I. A. eikonal is shown in fig. 4, where the curves computed with the values V=20 and 40 eV are reported. The V parameter acts in the sense of increasing the momenta of the interactingelectrons and thus affects both the momentum transfer and the momentum balance. However while the influence on the e-e scattering factor is mainly on the absolute value since its angular shape is only sligtly varied by V, the form factor is shrinked in to a smaller angular region. So that the overall effect is the analogous of having carried out measurements at an higher total energy. By choosing 20 eV as a value of the parameter, the D. W. I. A. eikonal fits the data quite well from 800 eV on, as can be seen in fig. 5. The distortion effects become almost negligible only from 1600 eV on, as shown in figs 6 and 7. It should be noted that, at least for the He system, the eikonal approximation, where V is taken equal to 20 eV is almost equivalent to a on shell I. A. description of the process.

A summary of the data taken at incident energies 800, 1600 and 2500 eV is reported in fig. 8. It shows a quite good agreement with the squared Fourier transform of the radial He 1s electron w. f. as computed by Clementi[12].

At variance in the out of plane geometry, for He, it is not necessary to use the D. W. I. A. to fit the data even at 200 eV incoming energy. This is because the e-e scattering factor is constant in that case and the distortion of the form factor results much smaller than in coplanar kinematics, as it is easily seen from the two different momentum reconstructions.

A behaviour analogous but somehow different to the one of He was found for the 2s electrons in Ne. The angular distribution taken at 800 eV disagrees with the one computed in eikonal D. W. I. A. V = 30 as shown in fig. 9. At the higher energies 1600 eV and 2600 eV (figs. 10 and 11) the eikonal D. W. I. A. appears to be valid. The agreement between the calculated Ne 2s Clementi w. f.[12] and the data is shown in fig. 12 for all the energies investigated.

The angular distribution arising from the Kr 4s electrons has been measured only for incident electron energy of 800 eV in coplanar symmetric geometry. It is reported in Fig. 13where it appears that the eikonal approximation with V=20 eV can fit the data. In fig. 14 the data have also been compared with the squared Fourier transform calculated by using the Kr 4s Clementi w. f.[12].

For the Xe 5s orbital the best fit to the data (fig. 15 and 16), is obtained in the distorted wave eikonal model, by putting V=10 eV in agreement with the smaller characteristic momentum of the bound electron. In fig. 17 data taken at 400, 800 and2600 eV incident electron energy are compared with the ϱ_{nl} obtained from the Xe 5s Clementi w. f.[12]. From all these data it appears that the characteristic momentum and the binding energy affect the range of validity of the models used in describing the scattering process.

As to the p electrons of Ne, Kr and Xe, the situation is not so simple. The computed shapes never appear in good agreementwith the data, even in the high energy range.

In particular in the case of the Ne 2p electrons (figs. 18 to 21), while the intensity ratios and the relative positions of maxima and minima are fairly well reproduced at energies larger than 1500 eV, at 800 eV the agreement fails at angles corresponding to low momentum transfer ($\vartheta \simeq 38^o$) both in coplanar symmetrical ($\vartheta_1 = \vartheta_2$) and asymmetrical ($\vartheta_1 \neq \vartheta_2$) geometry. All the data are reported in fig. 22 where, as usual, the comparaison between measured and calculated squared Fourier transform for the Ne 2p Clementi w. f.[12] is shown.

Data on the ejection of Kr 4p electrons are reported in the figs. 24, and 25 along with the comparaison (fig. 23) with the squared Fourier transform of the Kr 4p Clementi w.f.[12]. Also from these data it appears that at the lowest energies and small scattering angles ($\vartheta \leq 42^{o}$) the eikonal approximation cannot explain the data. A better agreement is obtained at higher energies.

Angular correlation of 5p electrons in Xe has been taken only at 400 eV as shown in fig. 26. At this energy the eikonal approximation fits partially the data. At small scattering angles the usual deficit of the measured cross section shows up again. Only the angular correlation obtained is reported and compared with curves belonging to different values of the V parameter for 5p Xe Clementi w.f.[12].

5. - CONCLUSIONS

From the analysis of these results, even if no absolute measurements of the cross section and of the spectroscopic factors have yet been carried out, some significant conclusions can be drawn on the check of the reaction mechanism and on the experimental conditions to be chosen to obtain the more reliable information on the atomic and molecular structure.

In coplanar geometry the conditions for the validity of the direct interaction without distortion, and hence for the (e, 2e) technique to be a good tool in testing a wave function, are satisfied for incoming electron energies quite high respect to the binding energy of the orbital under study and for momentum transfer large compared to the $\langle q \rangle$ momentum of the bound electron. In particular the P. W. I. A. model appears suitable to describe the (e, 2e) reactions in case of the external shells, for incoming electron energies of the order of 50 times the binding energy of the orbital and momenta transfer one order of magnitude ($\simeq 10$ times) larger than the $\langle q \rangle$ value.

For incident energies ranging from about 50 to about 20 times B_{nl} the eikonal D. W. I. A. can take care of the distortion effects and reliable information on the atomic and molecular orbitals can still be obtained.

For lower incident energies ($E_o \simeq 10\ B_{nl}$) more sophisticated models must be used in describing the scattering, so that, at this stage of the theory, experiments in this range of energy appear to be more useful in obtaining information about the reaction mechanism than in testing atomic w.f.s.

REFERENCES

(1) - R. Camilloni, A. Giardini Guidoni, G. Stefani and R. Tiribelli, Phys. Rev. Letters 29, 618 (1972)

(2) - S. T. Hood, I. E. Mc. Carthy, P. J. O. Teubner and E. Weigold Phys. Rev. A8, 2494 (1973)

(3) - A. Ugbabe, E. Weigold and I. E. Mc Carthy, Phys. Rev. A11, 576 (1975); E. Weigold, S. T. Hood and I. E. Mc. Carthy, Phys. Rev. A11, 566 (1975)

(4) - I. E. Mc. Carthy and E. Weigold to be published in Phys. Rept.

(5) - A. Giardini Guidoni, G. Missoni, R. Camilloni and G. Stefani in "Electron and Photon Interactions with Atoms" (Plenum Press, 1976) pag. 194 (H. Kleinpoppen and M. R. C. Mc. Dowell Editors).

(6) - G. Neudachin, G. A. Novoskol'tseva, Yu. F. Smirnov, Sov. Phys. JETP 28, 540 (1969).

(7) - S. T. Hood, A. Hamnett and C. E. Brion, Chem. Phys. Lett. 39, 252 (1976).

(8) - K. Jung, E. Schubert, D. A. L. Paul and H. Ehrahrdt, J. Phys. B. Atom. Molec. Phys. 8, 1330 (1975)

(9) - J. P. Coleman in "Case Studies in Atomic Collision Physics" (E. W. Mc Daniel and M. R. C. , Mc. Dowell Editors), (North Holland 1969) pag. 101.

(10) - R. Camilloni, G. Stefani, A. Giardini Guidoni, R. Tiribelli and D. Vinciguerra, Proceedings of the 5th Congress on Vacuum Science and Technology, Perugia (1975); A. Giardini Guidoni, R. Camilloni, G. Stefani, R. Tiribelli, D. Vinciguerra and E. Weigold, IX I. C. P. E. A. C. Seattle (1975) Abstract of papers, pag. 490, R. Camilloni, A. Giardini Guidoni, G. Stefani, R. Tiribelli and D. Vinciguerra, Chem. Phys. Letters 41, 17 (1976).

(11) - G. Baldacchini, Cryogenics 14, 574 (1974)

(12) - E. Clementi and C. Roetti, Atomic Data and Nuclear Data Tables 14, 177 (1974).

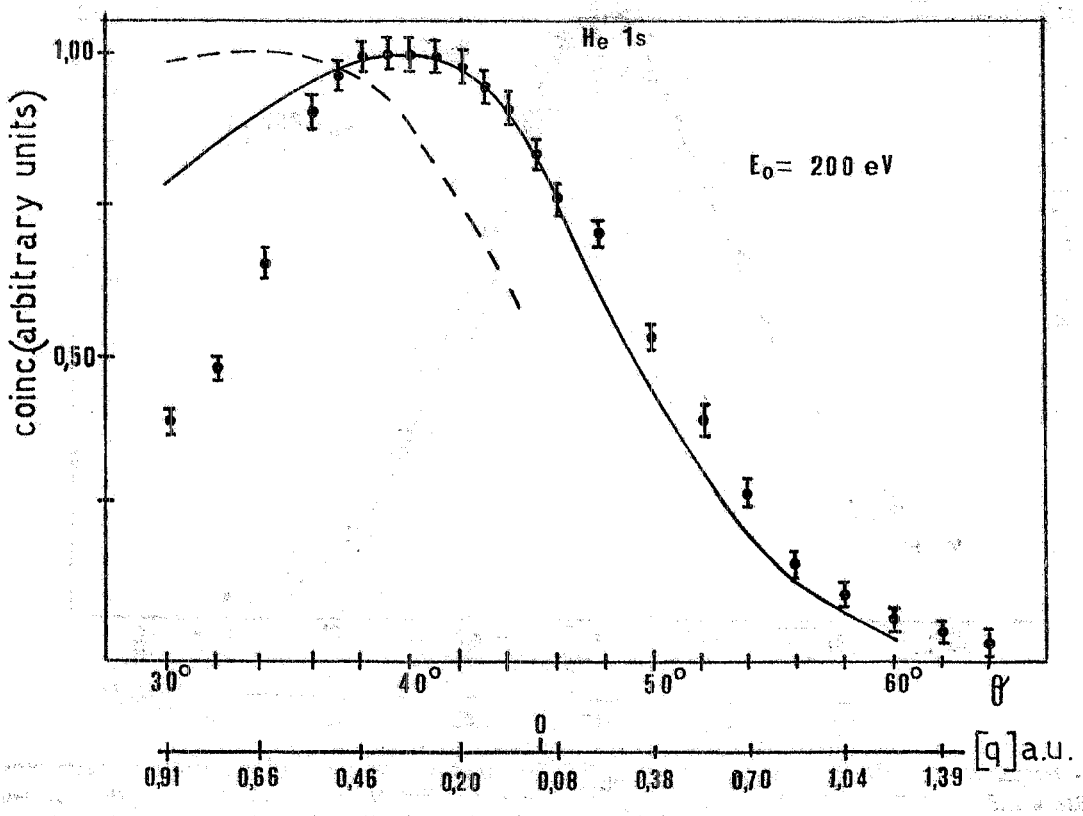

Fig. 3 - Angular correlation for the 1s orbital of He. Measured coincidence rate is compared with shapes calculated for the 1s Clementi wave function in P.W.I.A. (---) and D.W.I.A. (eikonal V=20 eV) (——). The correspondence between scattering angle and [q] value determined from V=20 eV is also reported.

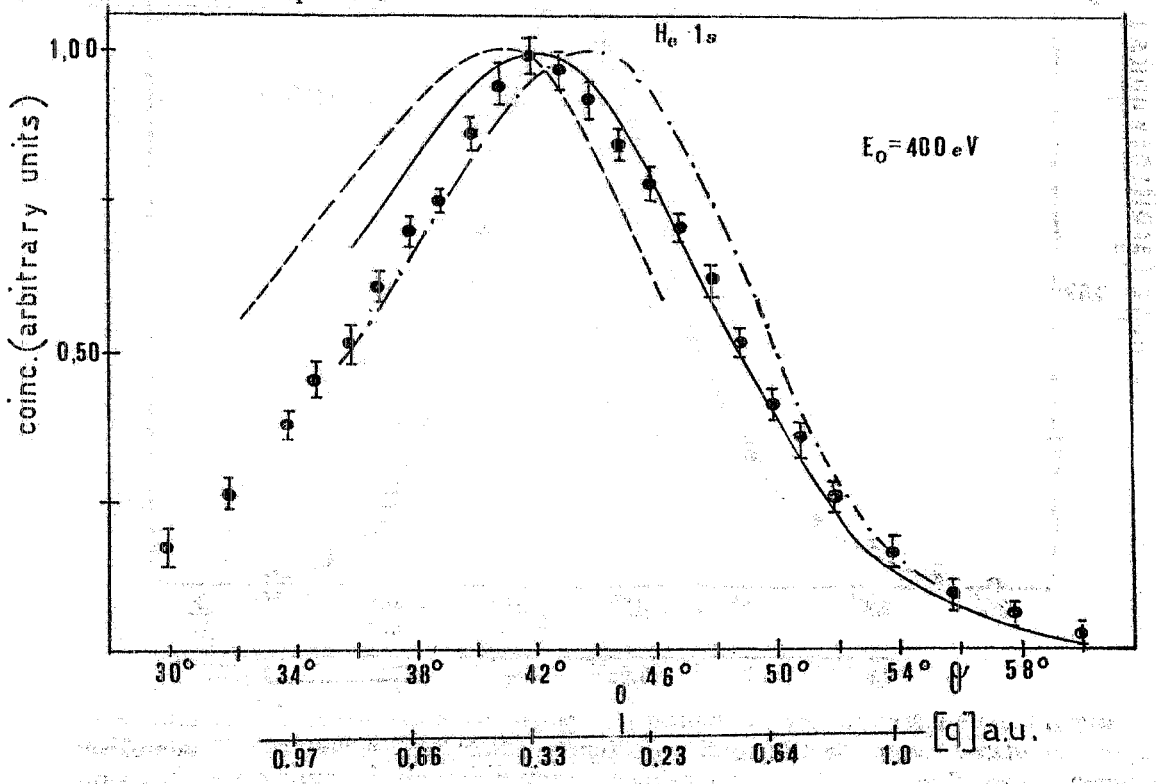

Fig. 4 - Angular correlation for the 1s orbital of He. Measured coincidence rate is compared with shapes calculated for 1s Clementi wave function in P.W.I.A. (---) and D.W.I.A. (eikonal V=20 eV) (——) and V=40 eV (-·-·-). The correspondence between scattering angle and [q] value determined from V=20 eV is also reported.

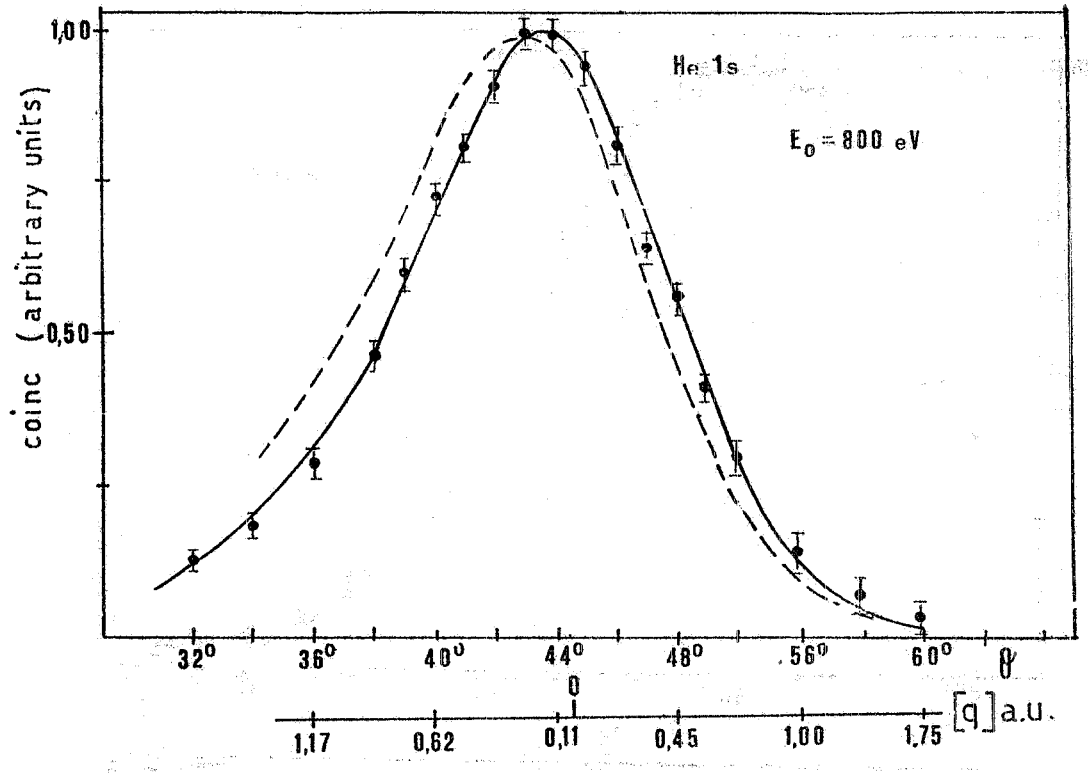

Fig. 5 - Angular correlation for the 1s orbital of He. Measured coincidence rate is compared with shapes calculated for the 1s Clementi wave function in P.W.I.A. (---) and D.W.I.A. (eikonal V=20 eV) (——). The correspondence between scattering angle and [q] value determined from V=20 eV is also reported.

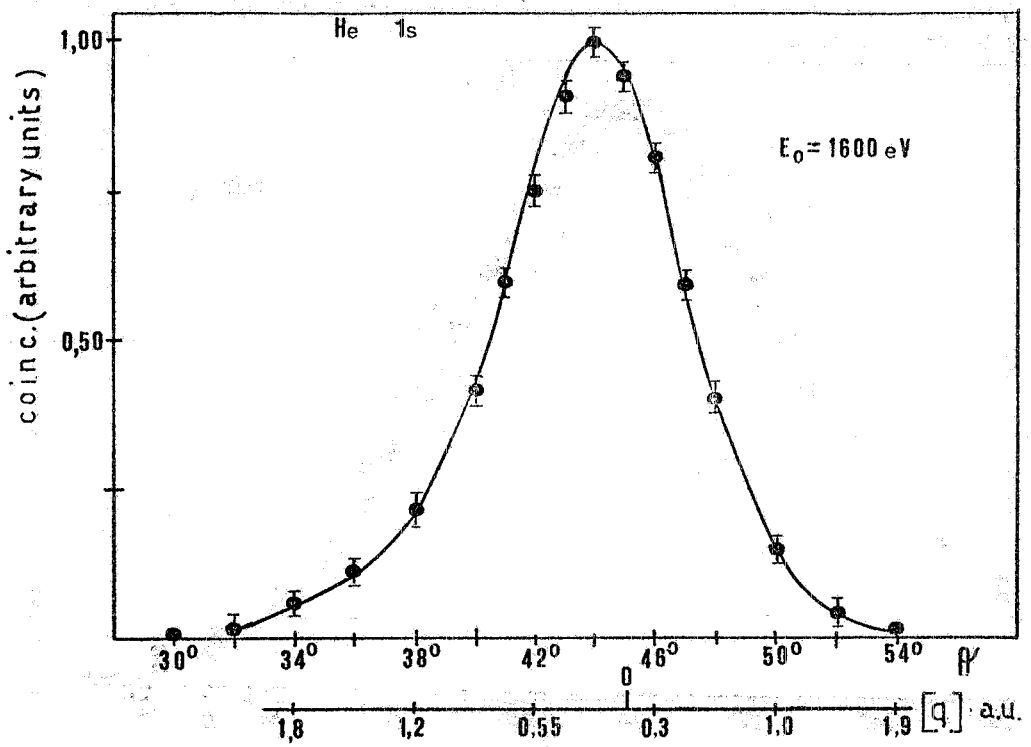

Fig. 6 - Angular correlation for the 1s orbital He. Measured coincidence rate is compared with shapes calculated for the 1s Clementi wave function in D.W.I.A. (eikonal V=20 eV) (indistinguishable from P.W.I.A. The correspondence between scattering angle and [q] value determined from V=20 eV is also reported.

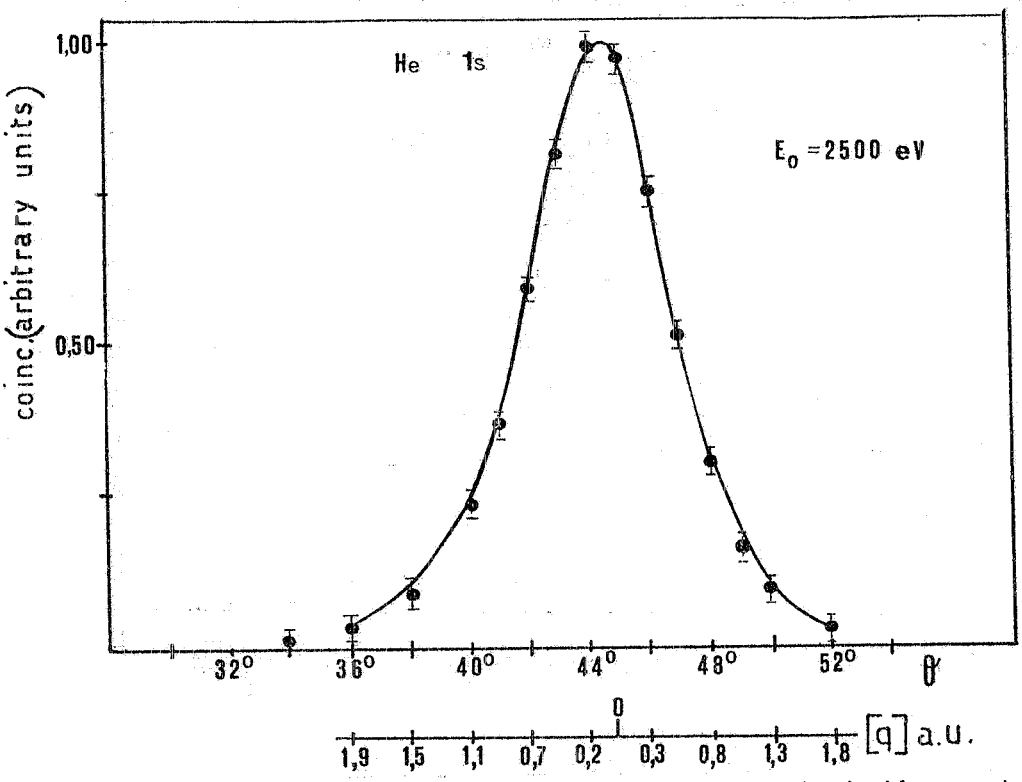

Fig. 7 - Angular correlation for the 1s orbital of the He. Measured coincidence rate is compared with shapes calculated for the 1s Clementi wave function D.W.I.A. (eikonal V=20 eV) indistinguishable from P.W.I.A. The correspondance between scattering angle and [q] value determined from 20 eV is also reported.

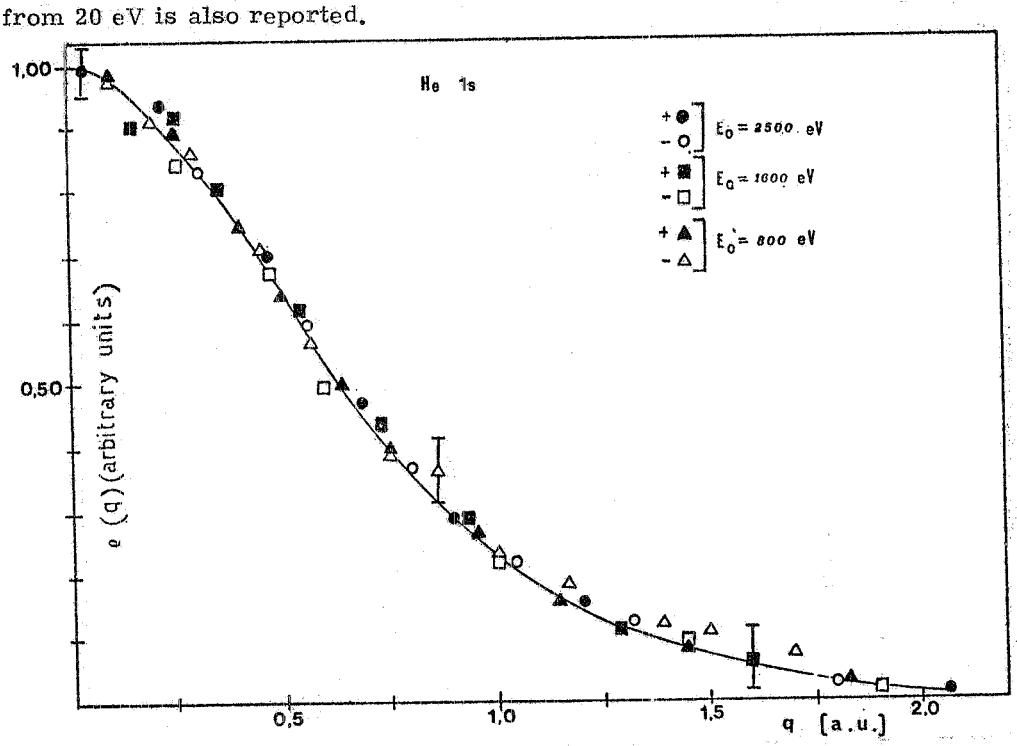

Fig. 8 - q distribution resulting in D.W.I.A. (eikonal V=20 eV) in coplanar symmetrical conditions for incident electron energies of 800, 1600 and 2500 eV. The full curve is the squared Fourier transform of the He 1s Clementi wave function to which the data have been normalized. (Open marks are relative to [-q] antiparallel to the momentum of the incoming electron). B_{n1} optical = 24.58 eV.

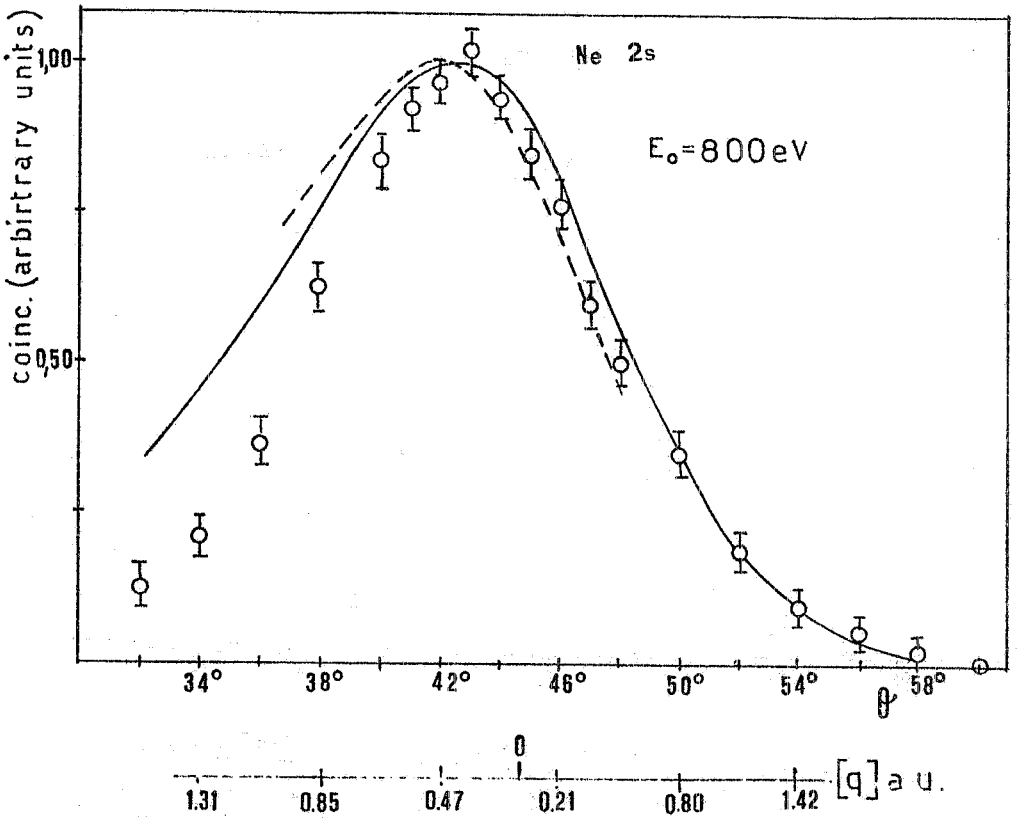

Fig. 9 - Angular correlation for the 2s orbital of Ne. Measured coincidence rate is compared with curves calculated for the Ne 2s Clementi wave function in P.W.I.A. (---) and D.W.I.A. (eikonal V=30 eV) (——). The correspondence between scattering angle and [q] value determined from V=30 eV is also reported in the lower scale.

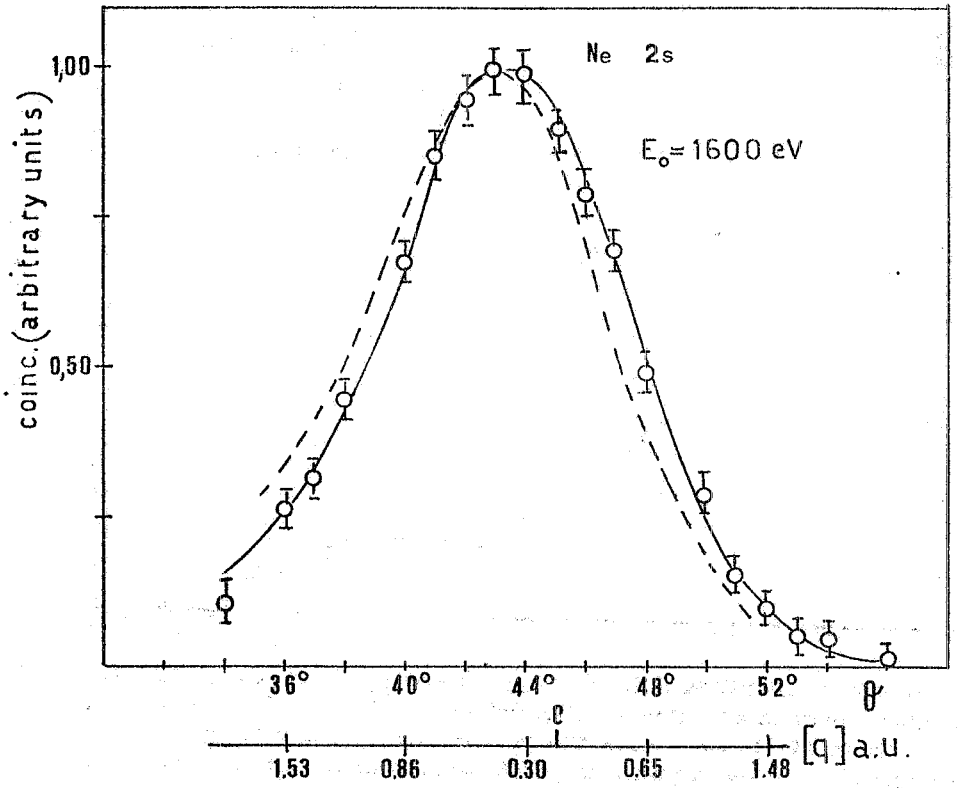

Fig. 10 - Angular correlation for the 2s orbital of Ne. Measured coincidence rate is compared with curves calculated for the Ne 2s Clementi wave function in P.W.I.A. (---) and D.W.I.A. (eikonal V=30 eV) (——). The correspondence between scattering angle and [q] value determined from V=30 eV is also reported in the lower scale.

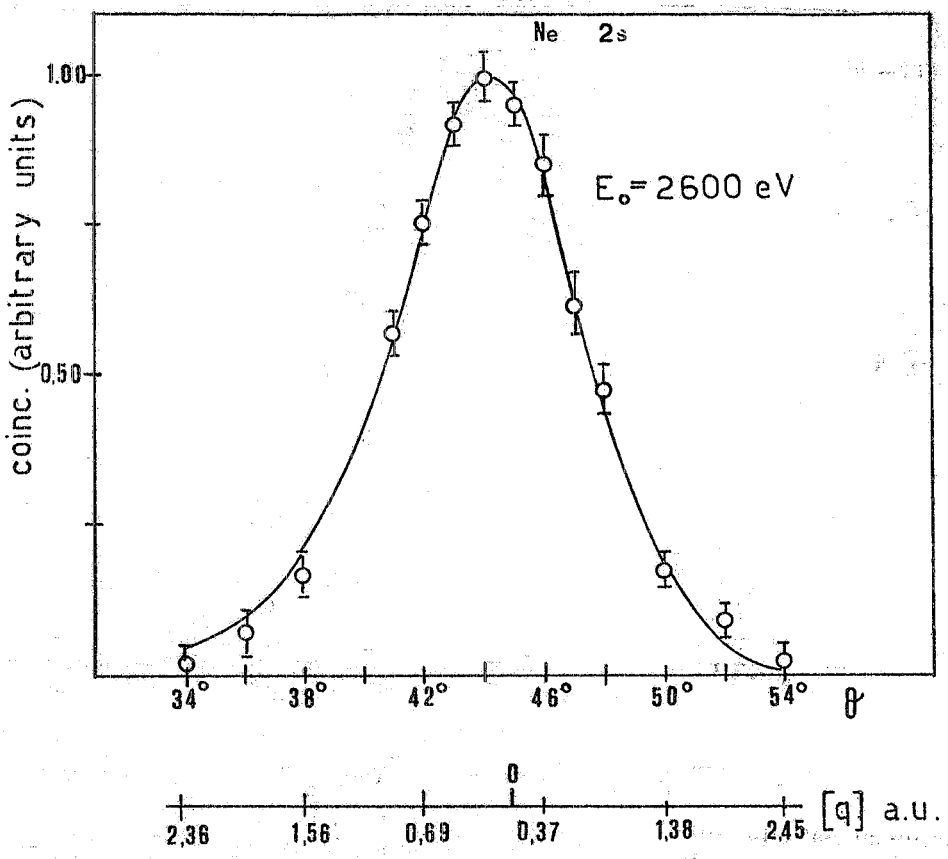

Fig. 11 - Angular correlation for the 2s orbital of Ne. Measured coincidence rate is compared with curves calculated for the Ne 2s Clementi wave function in D.W.I.A. (eikonal V=30 eV) almost indistinguishable from P.W.I.A.. The correspondence between scattering angle and [q] value determined from V=30 eV is also reported in the lower scale.

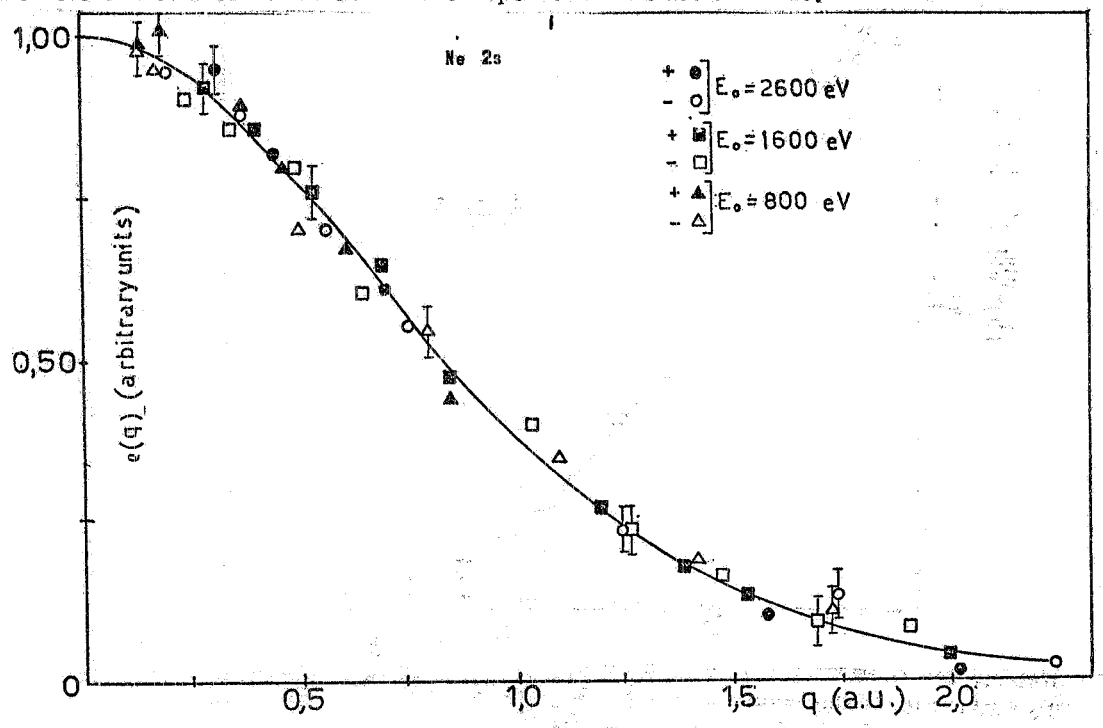

Fig. 12 - q distribution resulting in D.W.I.A. (eikonal V=30 eV) in coplanar symmetrical conditions for incident electron energies of 2600, 1600 and 800 eV (for $\vartheta > 42^o$). The full curve is the squared Fourier transform of the Ne 2s Clementi w.f. to which the data have been normalized (Open marks are relative to [q] antiparallel to the momentum of the incoming electron). B_{nl} optical = 48.5 eV.

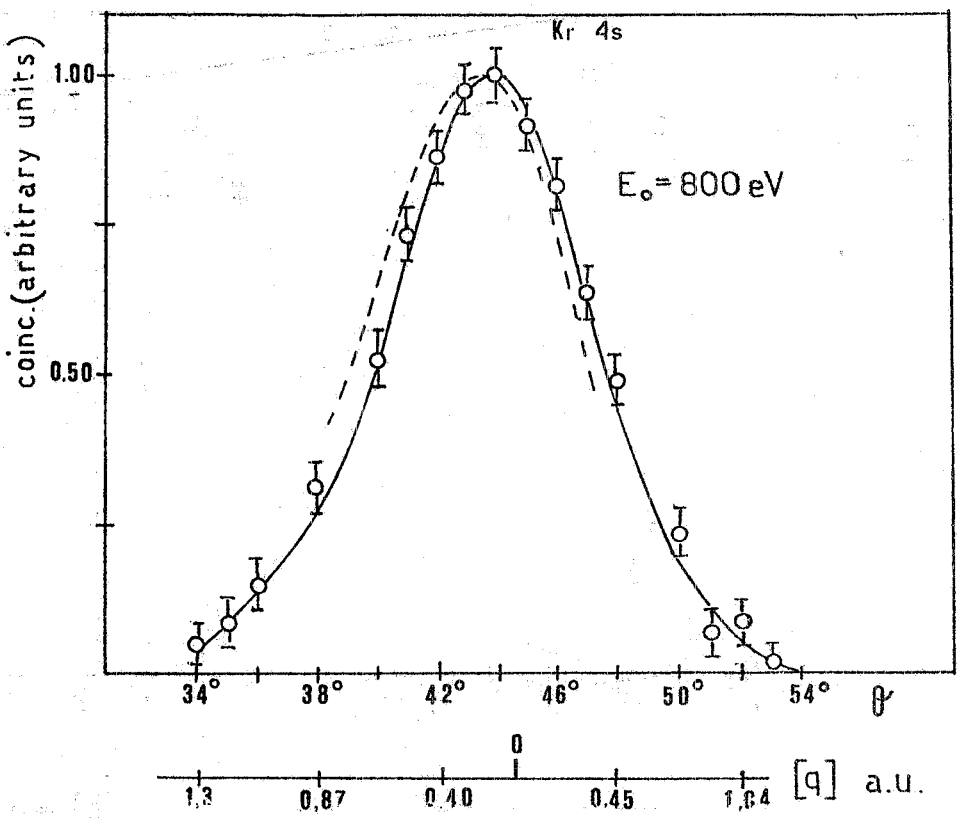

Fig. 13 - Angular correlation for the 4s orbital of Kr (B_{nl} = 27.5 eV). Measured coincidence rate is compared with curves calculated for the Kr 4s Clementi wave function in P.W.I.A. (---) and D.W.I.A. (——) (eikonal V=20 eV). The correspondence between scattering angle and [q] values determined from V=20 is also reported.

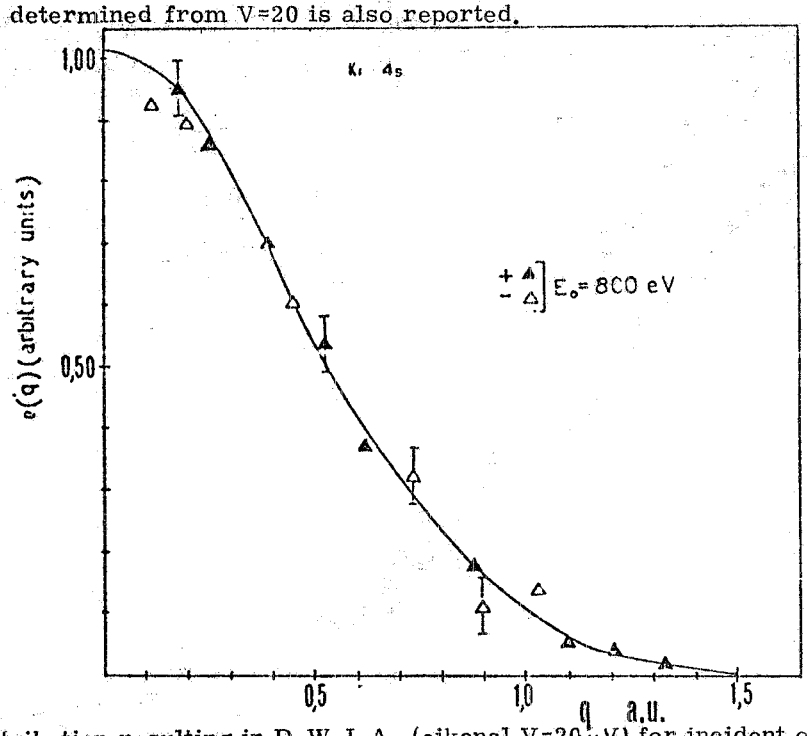

Fig. 14 - q distribution resulting in D.W.I.A. (eikonal V=20 eV) for incident electron energy of 800 eV. The full curve is the squared Fourier transform of the Kr. 4s Clementi w.f. to which the data have normalized. B_{nl} optical = 27.51 eV.

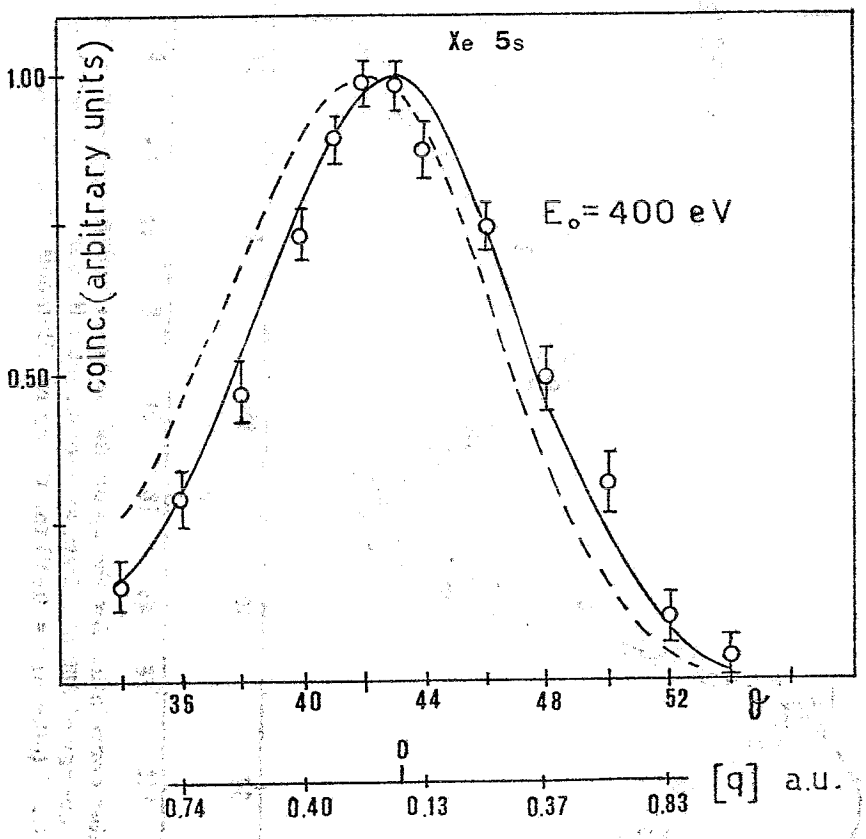

Fig. 15 - Angular correlation for the 5s orbital of Xe. Measured coincidence rate is compared with curves calculated for the Xe 5s Clementi wave function in P.W.I.A. (---) and D.W.I.A. (——) (eikonal V=10 eV). The correspondence between scattering angle and [q] value is in the lower scale.

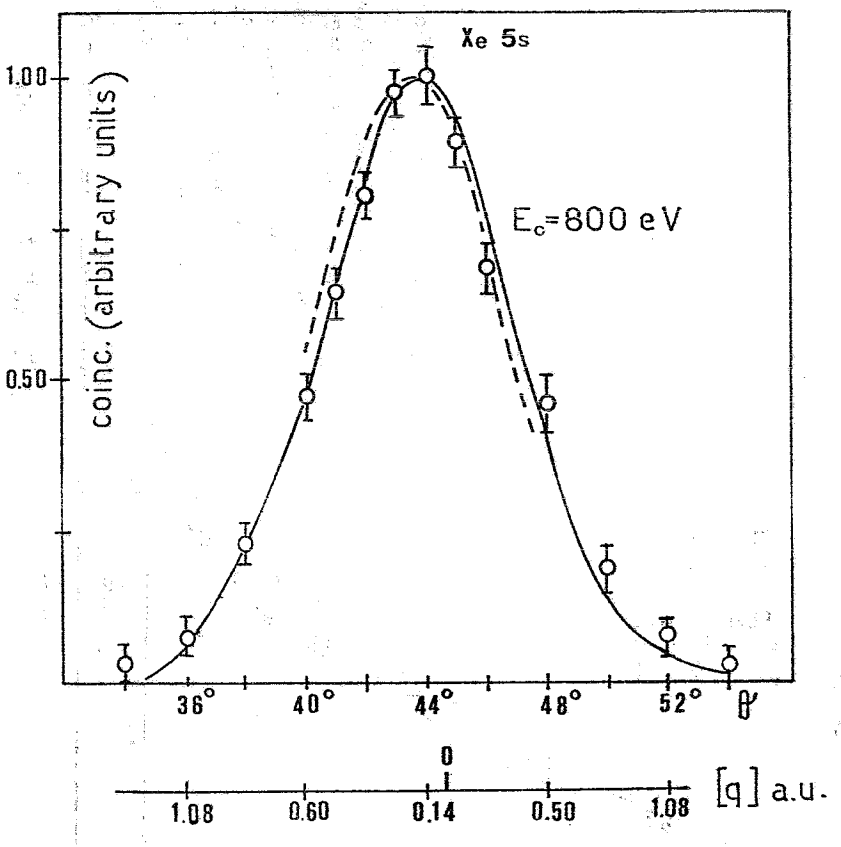

Fig. 16 - Angular correlation for the 5s orbital of Xe. Measured coincidence rate is compared with curves calculated for the 5s Clementi wave function in P.W.I.A. (---) and D.W.I.A. (——) (eikonal V=10 eV). The correspondance scattering angle and [q] value is in the lower scale.

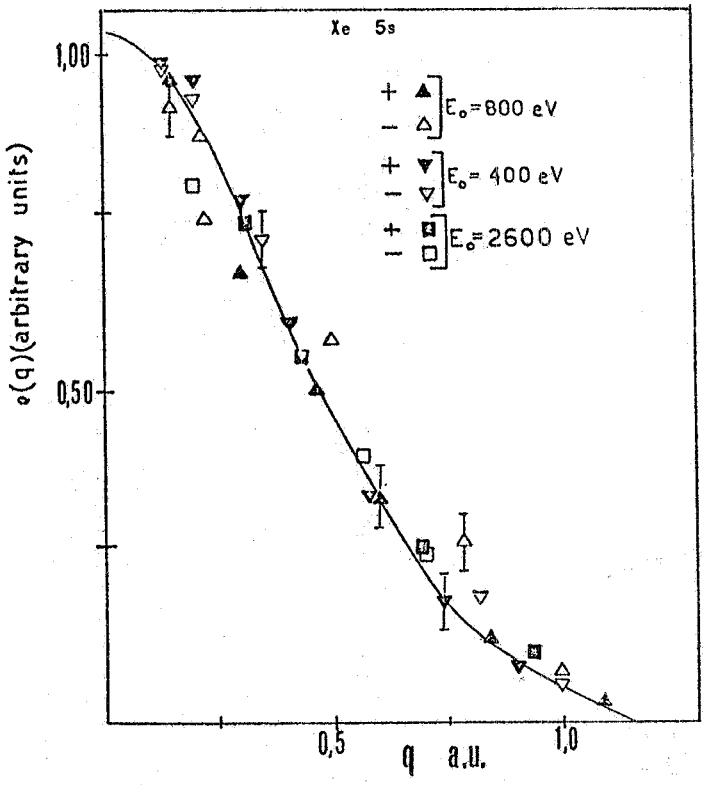

Fig. 17. - q distribution resulting in D. W. I. A. (eikonal V=10 eV) in coplanar symmetrical conditions for incident electron energies of 400, 800 and 2600 eV. The full curve is the squared Fourier transform of Xe 5s double zeta Clementi w. f. to which the data have been normalized (Open marks are relative to q antiparallel to the momentum of the incoming electron). B_{nl} optical=23, 40 eV.

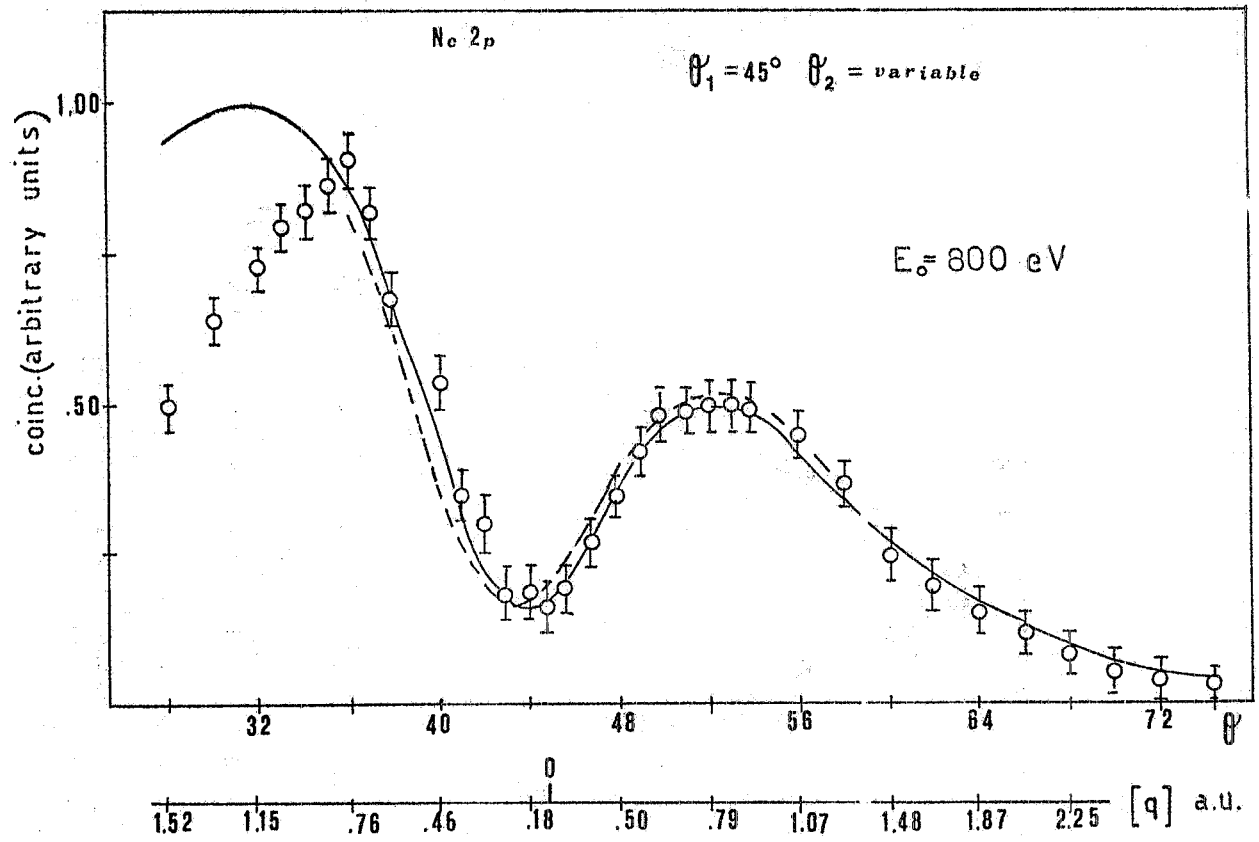

Fig. 18 - Angular correlation for the 2p orbital of Ne in coplanar asymmetrical geometry for incident electron energy of 800 eV. Data are compared with curves calculated in P. W. I. A. (---) and D. W. I. A. (——) (eikonal V=10 eV) for the 2p Ne Clementi wave function.

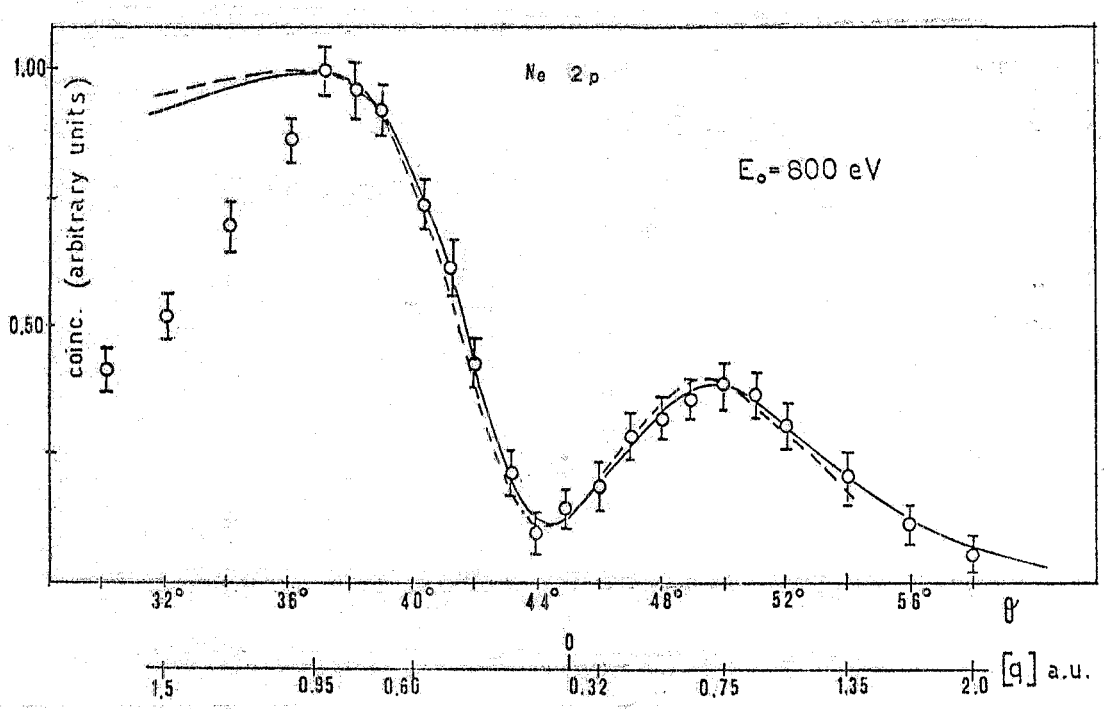

Fig. 19 - Angular correlation for the 2p orbital of Ne measured in coplanar symmetrical geometry at incident electron energy of 800 eV. Data are compared with shapes calculated in P.W.I.A. (---) and D.W.I.A. (——) (eikonal V=10 eV) for the 2p Ne Clementi wave function.

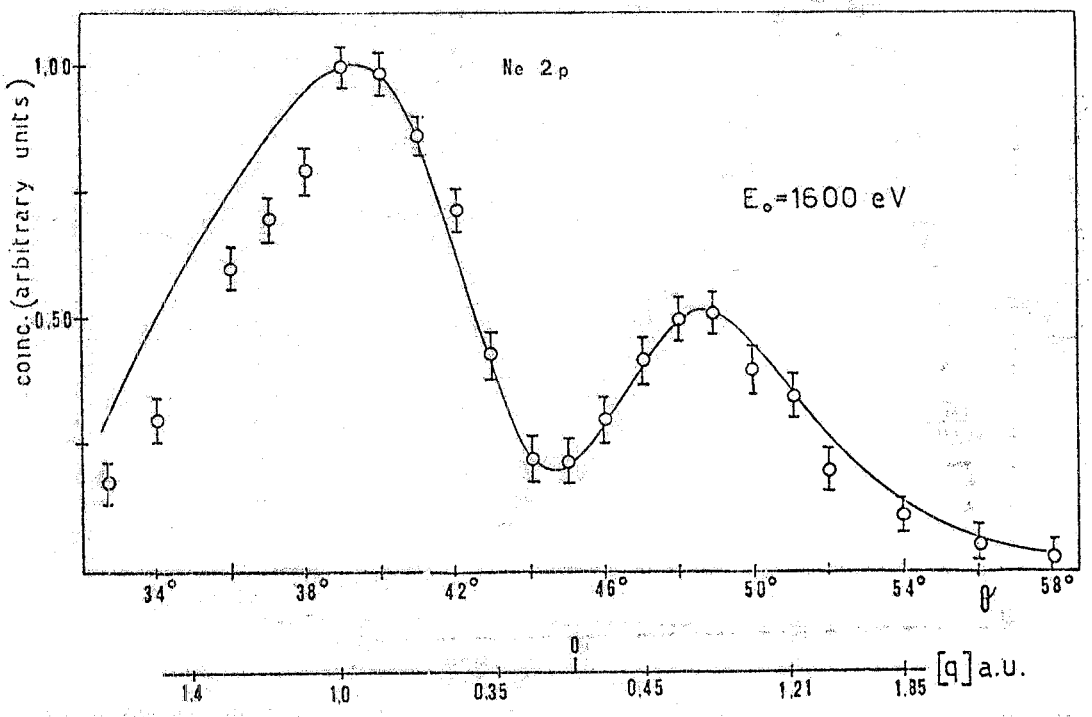

Fig. 20 - Angular correlation for the 2p orbital of Ne measured in coplanar symmetrical geometry at incident electron energy 1600 eV. Data are compared with a curve calculated for 2p Ne Clementi w.f. in P.W.I.A. almost indistinguishable from D.W.I.A. (eikonal V=10 eV).

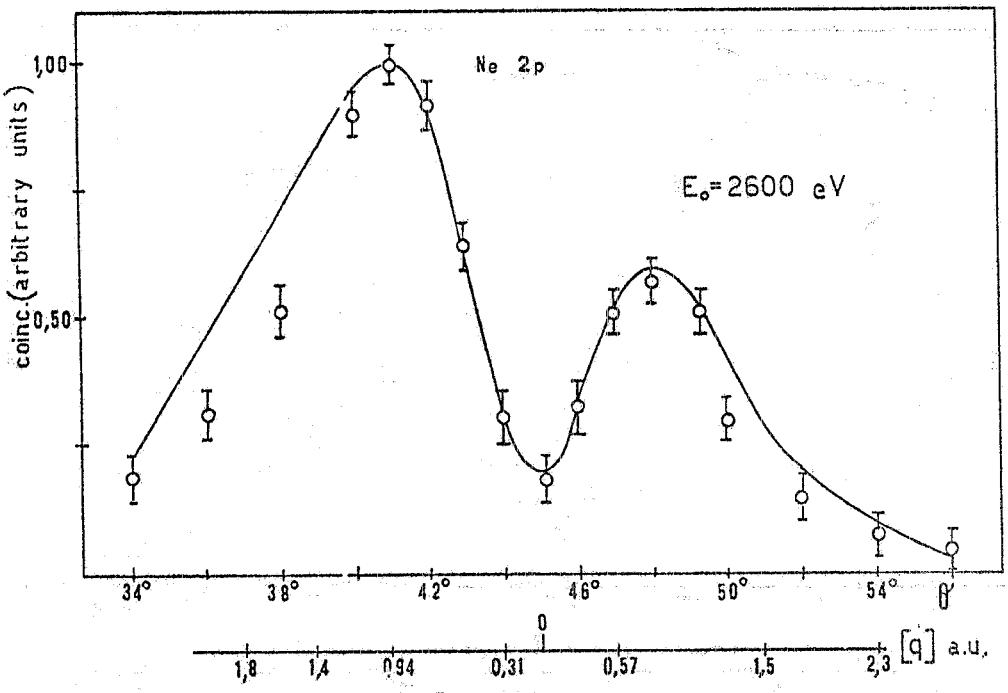

Fig. 21 - Angular correlation for the 2p orbital of Ne measured in coplanar symmetrical conditions at incident electron energy of 2600 eV. Data are compared with a curve calculated for the 2p Ne Clementi w.f. in P.W.I.A. almost indistinguishable from D.W.I.A. (eikonal V=10 eV).

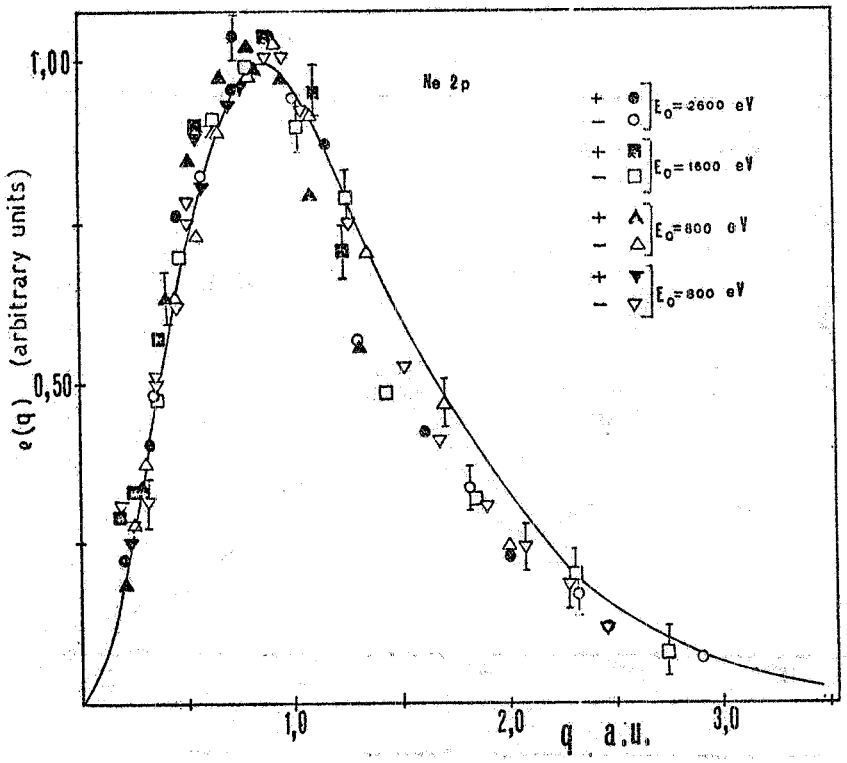

Fig. 22 - q distribution resulting in D.W.I.A. (eikonal V=10 eV) in coplanar symmetrical and asymmetrical conditions for incident electron energies of 800, 1600 and 2600 eV. The full curve is the squared Fourier transform of the Ne 2p Clementi w.f. to which the data have been normalized (open marks are relative to [q] antiparallel to the momentum of the incoming electron). B_{nl} optival = 21.59 eV.

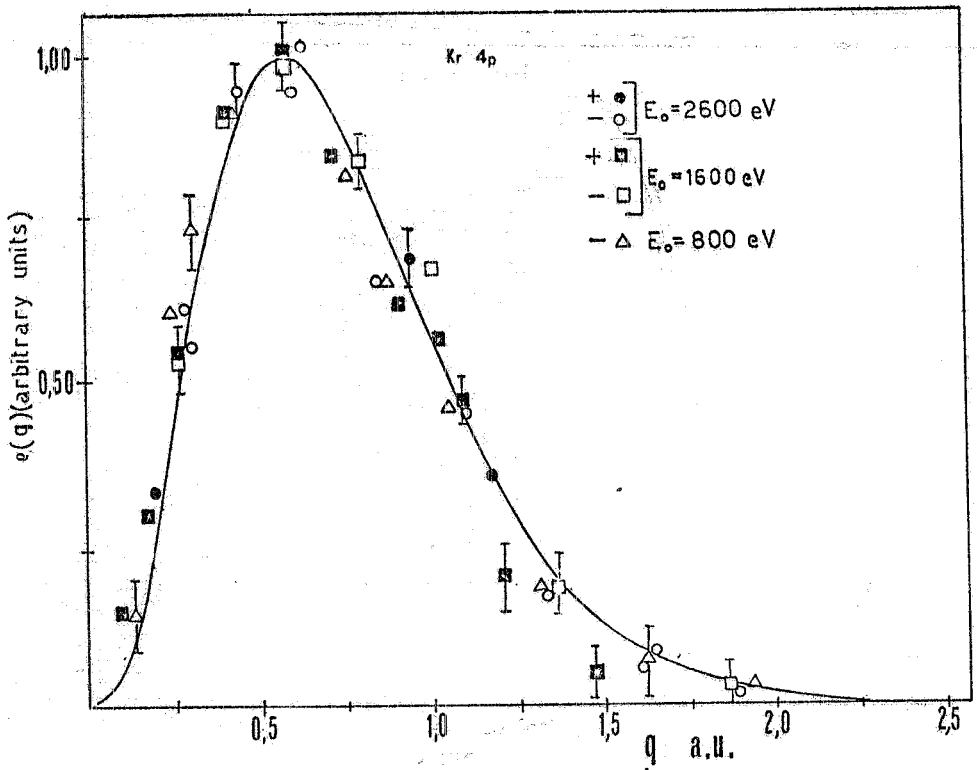

Fig. 23 - q distribution resulting in D.W.I.A. (eikonal V=15 eV) in coplanar symmetrical conditions for incident electron energies of 800 ($\vartheta > 42^{o}$), 1600 and 2600 eV. B_{nl} optical = 14.00 eV.

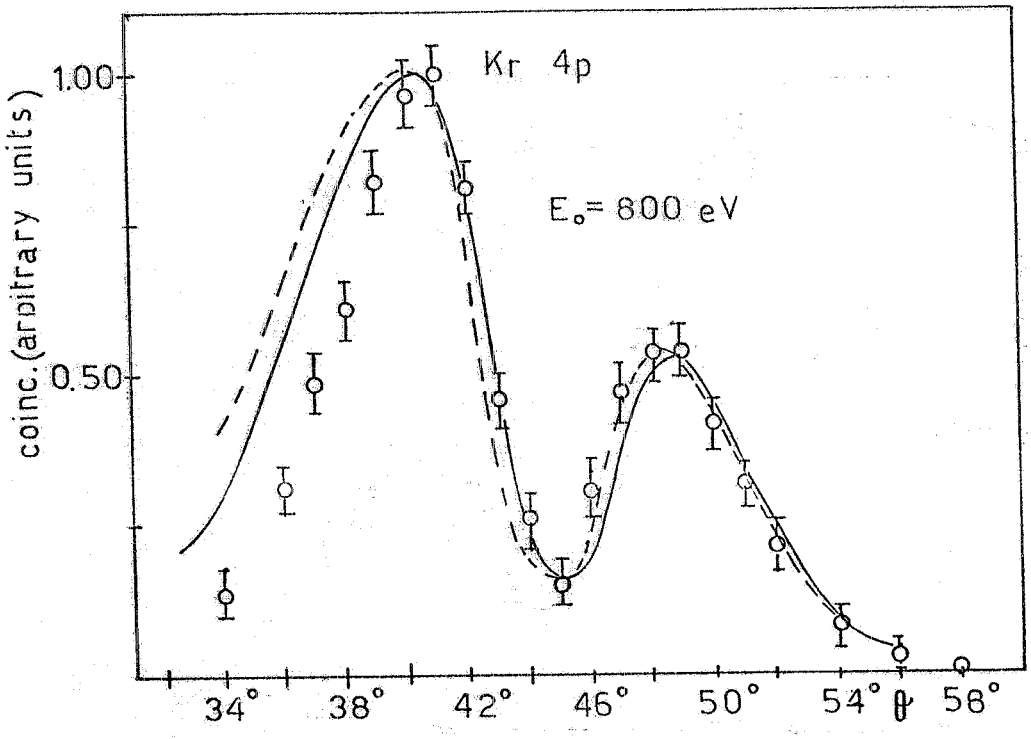

Fig. 24 - Angular correlation for the ejection of the 4p electrons in Kr at incident electron energy of 800 eV. Comparison is made with curves calculated in P.W.I.A. (---) and eikonal approximation with V=15 eV (——) for the Kr 4p Clementi w.f.

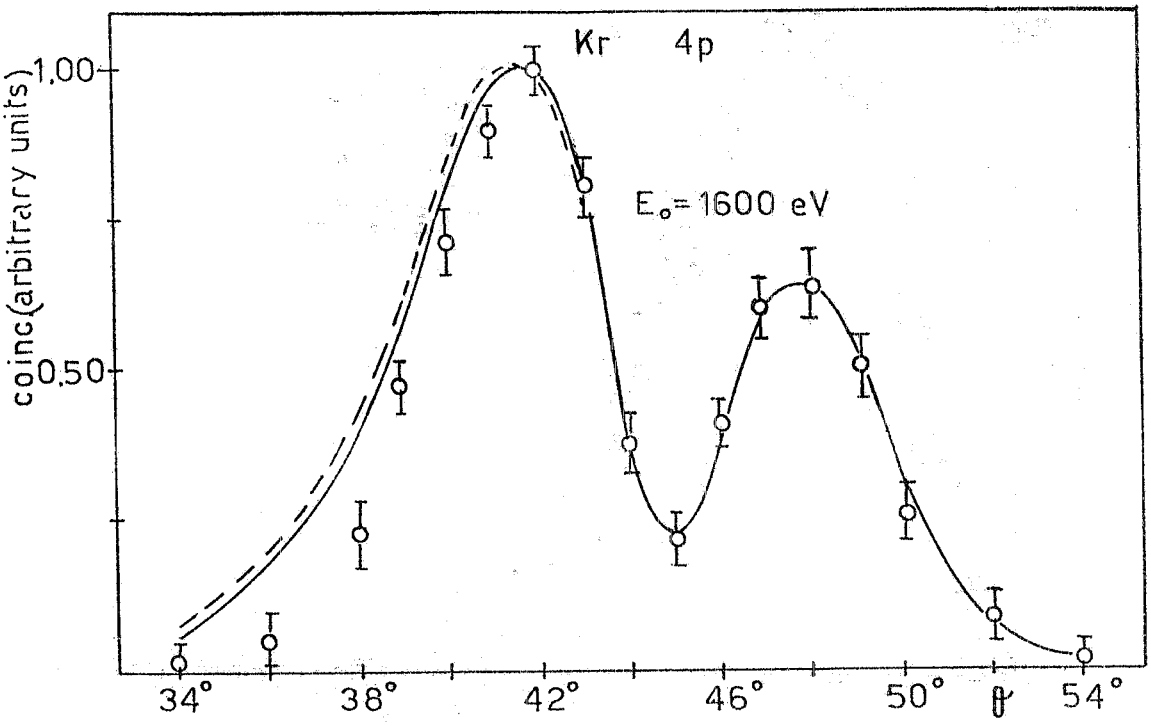

Fig. 25 - Angular correlation for the 4p orbital in Kr taken at incoming electron energy of 1600 eV compared with curves calculated in P.W.I.A. (---) and D.W.I.A. (——) (eikonal V= = 15 eV) for the Kr 4p Clementi w.f.

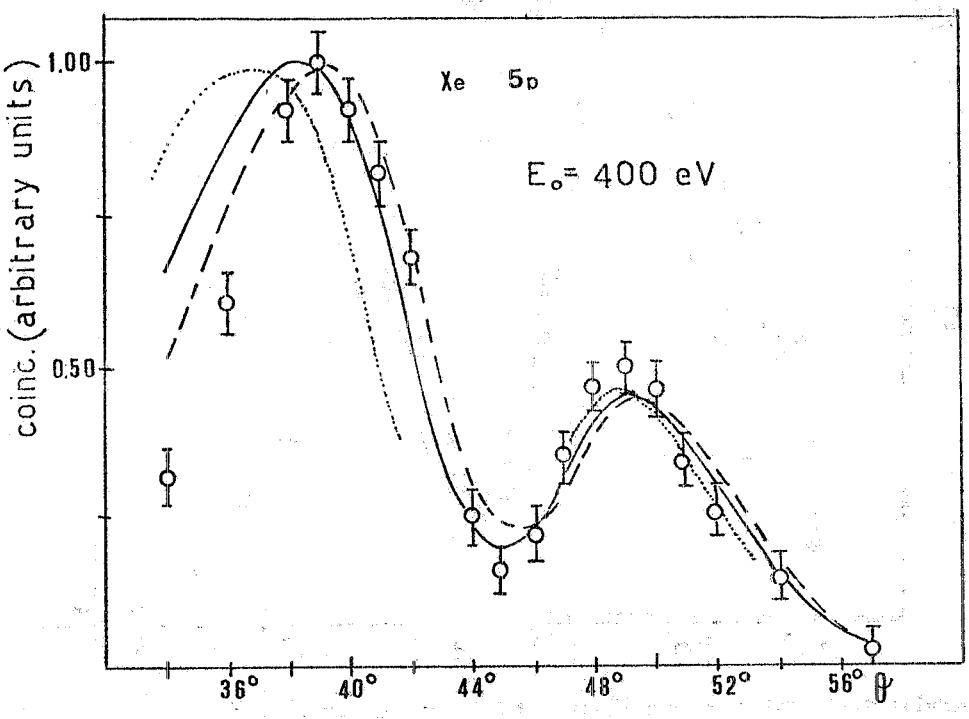

Fig. 26 - Angular correlation observed in the ejection of Xe 5p electrons at incident energy of 400 eV. Data are compared with curves calculated in P.W.I.A. (···), eikonal approximation (V=10 eV) (——) and V=20 eV (---) for the Xe 5p double zeta Clementi wave function. B_{nl} optical = 12.13 eV.